

# Complex magnetic ordering in $\text{EuAl}_4$ -A $^{151}\text{Eu}$ Mössbauer study

Cite as: AIP Advances 14, 015239 (2024); doi: 10.1063/9.0000621  
Submitted: 11 September 2023 • Accepted: 27 November 2023 •  
Published Online: 23 January 2024



D. H. Ryan,<sup>1,a)</sup> Brinda Kuthanazhi,<sup>2,3</sup> Na Hyan Jo,<sup>2,3,b)</sup> and Paul C. Canfield<sup>2,3</sup>

## AFFILIATIONS

<sup>1</sup> Physics Department and Centre for the Physics of Materials, McGill University, 3600 University Street, Montreal, QC H3A 2T8, Canada

<sup>2</sup> Ames National Laboratory, U.S. Department of Energy, Iowa State University, Ames, Iowa 50011-3020, USA

<sup>3</sup> Department of Physics and Astronomy, Iowa State University, Ames, Iowa 50011, USA

**Note:** This paper was presented at the 68th Annual Conference on Magnetism and Magnetic Materials.

<sup>a)</sup> Author to whom correspondence should be addressed: [dhryan@physics.mcgill.ca](mailto:dhryan@physics.mcgill.ca)

<sup>b)</sup> Current address: Department of Physics, University of Michigan, Ann Arbor, MI 48109-1040

## ABSTRACT

$^{151}\text{Eu}$  Mössbauer spectroscopy has been used to investigate the behaviour of  $\text{EuAl}_4$  through the four magnetic transitions that occur below 16 K. We find clear evidence for the first transition ( $T_{N1}$ , the onset of order) where an incommensurate modulated magnetic structure appears, and the third ( $T_{N3}$ ) where the modulation disappears at the tetragonal  $\rightarrow$  orthorhombic structural transition. We see no changes at the lowest transition ( $T_{N4}$ ) but find that the modulation amplitude passes through a maximum at  $T_{N2}$ . Data on the isostructural but magnetically simpler  $\text{EuGa}_4$  are also presented for comparison.

© 2024 Author(s). All article content, except where otherwise noted, is licensed under a Creative Commons Attribution (CC BY) license (<http://creativecommons.org/licenses/by/4.0/>). <https://doi.org/10.1063/9.0000621>

## I. INTRODUCTION

Both  $\text{EuAl}_4$  and  $\text{EuGa}_4$  adopt the same tetragonal  $\text{BaAl}_4$ -type structure ( $I4/mmm$  No. 139) with the europium atoms on the  $2a$  site forming a  $bct$  lattice.<sup>1</sup> Whereas  $\text{EuGa}_4$  exhibits simple basal-plane antiferromagnetic (AFM) ordering below  $T_N = 16.5$  K,<sup>2</sup> with the body centre moments antiparallel to the corner ones,<sup>3</sup>  $\text{EuAl}_4$  undergoes a complex sequence of four magnetic transitions below 16 K.<sup>4</sup> Time-of-flight Laue neutron diffraction identified an incommensurate  $(\delta_2, \delta_2, 0)$  magnetic structure below  $T_{N1} = 15.4$  K with a change to  $(\delta_1, 0, 0)$  at  $T_{N3} = 12.2$  K, but saw no distinct changes at either  $T_{N2} = 13.2$  K or  $T_{N4} = 10.0$  K.<sup>5</sup>

Here we study flux-grown  $\text{EuAl}_4$  and  $\text{EuGa}_4$  using  $^{151}\text{Eu}$  Mössbauer spectroscopy to observe the spectral changes at the four magnetic transitions. We find that  $\text{EuAl}_4$  adopts an incommensurate modulated magnetic structure, and as with the earlier Laue neutron diffraction work,<sup>5</sup> we find clear changes at  $T_{N1}$  and  $T_{N3}$ , but nothing at  $T_{N4}$ . The evolution of the order on warming from  $T_{N3}$  to  $T_{N1}$  appears to involve a progressive rounding of the modulation as it becomes more sinusoidal in nature, with the amplitudes

of the modulation passing through a maximum at  $T_{N2}$ . Data on the isostructural  $\text{EuGa}_4$  are also presented as an example of simpler behaviour.

## II. EXPERIMENTAL METHODS

Single crystal samples of  $\text{EuAl}_4$  and  $\text{EuGa}_4$  were grown from excess Al and Ga respectively. Starting compositions of  $\text{EuAl}_9$  and  $\text{EuGa}_9$  were loaded into fritted alumina Canfield crucible sets (CCS)<sup>6,7</sup> and sealed in fused silica tubes with a partial pressure of helium. Typical growth conditions were an homogenising anneal at 1000 °C for 3 h followed by a 200 h cool to 660 °C ( $\text{EuAl}_4$ ) or 400 °C ( $\text{EuGa}_4$ ), after which the excess flux was removed by centrifuging.<sup>8</sup> Faceted mm-sized crystals were obtained in both cases, and phase identity was confirmed by Cu-K $\alpha$  powder x-ray diffraction. Derived lattice parameters given in Table I are consistent with previous reports.<sup>2,4</sup>

$^{151}\text{Eu}$  Mössbauer spectroscopy measurements were carried out on a conventional spectrometer driven in sinusoidal mode and calibrated using a standard  $^{57}\text{CoRh}/\alpha\text{-Fe}$  foil. Isomer shifts are quoted

**TABLE I.** Summary of fitted ambient temperature lattice parameters and  $^{151}\text{Eu}$  Mössbauer spectral parameters [Isomer shift ( $\delta$ ) and hyperfine field ( $B_{hf}$ )] at 5 K. The quadrupole contribution ( $\Delta$ ) in both cases is taken from spectra in the paramagnetic state just above the magnetic transition temperature. Fitted transition temperatures for  $\text{EuAl}_4$  and  $\text{EuGa}_4$  are also given. Note:  $\text{EuGa}_4$  only has a single antiferromagnetic transition.

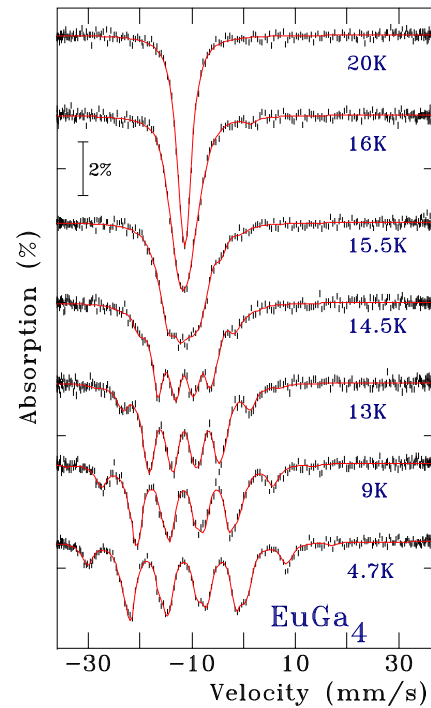
	$\text{EuAl}_4$	$\text{EuGa}_4$
$a$ (Å)	4.404 01(5)	4.407 12(6)
$c$ (Å)	11.175 26(16)	10.688 83(18)
$\delta$ (mm/s)	-10.75(2)	-11.35(2)
$\Delta$ (mm/s)	5.5(3)	6(1)
$B_{hf}$ (T)	26.55(4)	26.56(6)
$T_N$ (K)	...	16.25(3)
$T_{N3}$ (K)	12.0(2)	...
$T_{N2}$ (K)	13.4(2)	...
$T_{N1}$ (K)	15.7(1)	...

relative to  $\text{EuF}_3$  at ambient temperature. Samples were cooled in a vibration-isolated closed-cycle helium refrigerator. The simpler spectra were fitted to a sum of Lorentzian lines with the positions and intensities derived from a full solution to the nuclear Hamiltonian.<sup>9</sup> In cases where an incommensurate modulated magnetic structure was observed, the spectra were fitted using a distribution of hyperfine fields ( $B_{hf}$ ) derived from an (assumed) sinusoidal modulation of the moments.<sup>10,11</sup> Departure from a purely sinusoidal modulation was allowed for by including higher harmonics ( $Bk_3$ , etc.) of the fundamental  $Bk_1$ . A constant term ( $Bk_0$ ) was included to model the fully square-wave final state.

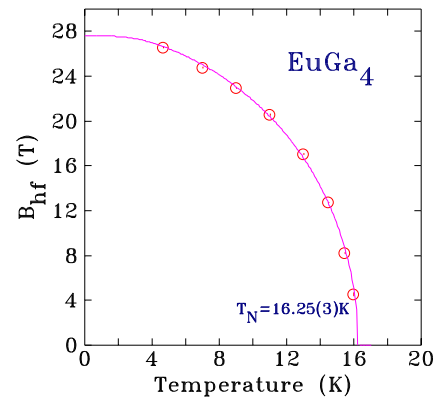
### III. RESULTS

#### A. $\text{EuGa}_4$

We first present data for  $\text{EuGa}_4$  as it provides an example of simple behaviour against which the more complex behaviour of  $\text{EuAl}_4$  can be more fully appreciated. The spectra in Fig. 1 show the steady development of magnetic splitting on cooling through  $T_N$ , and as Fig. 2 shows, the evolution of  $B_{hf}$  closely follows the expected  $J = \frac{7}{2}$  mean-field behaviour giving a transition temperature of  $T_N = 16.25(3)$  K, consistent with Homma *et al.*<sup>12</sup> In addition, three of the four strongest peaks are visibly split due to the effects of the quadrupole contribution ( $\Delta$ ). More correctly, each of the observed “peaks” in a magnetically split  $^{151}\text{Eu}$  Mössbauer spectrum results from several unresolved contributions from the eighteen allowed transitions between the  $I_e = \frac{7}{2}$  excited state and the  $I_g = \frac{5}{2}$  ground state. The effects of  $\Delta$  here partially separate some of those overlapping peaks. The uncertainty on  $\Delta$  is relatively large as it is small and only causes a slight asymmetry in a paramagnetic  $^{151}\text{Eu}$  Mössbauer spectrum. Fitting the 4.7 K spectrum places the  $B_{hf}$  approximately perpendicular to  $V_{ZZ}$ .<sup>13</sup> Since the  $4/mmm$  point symmetry of the  $2a$  site occupied by europium in  $\text{EuGa}_4$  forces the principal axis of the electric field gradient tensor,  $V_{ZZ}$ , to lie along the crystallographic  $c$ -axis, this indicates that the europium moments lie in the basal plane, consistent with the magnetic structure determined by neutron diffraction,<sup>3</sup> and earlier  $^{151}\text{Eu}$  Mössbauer work.<sup>12</sup>



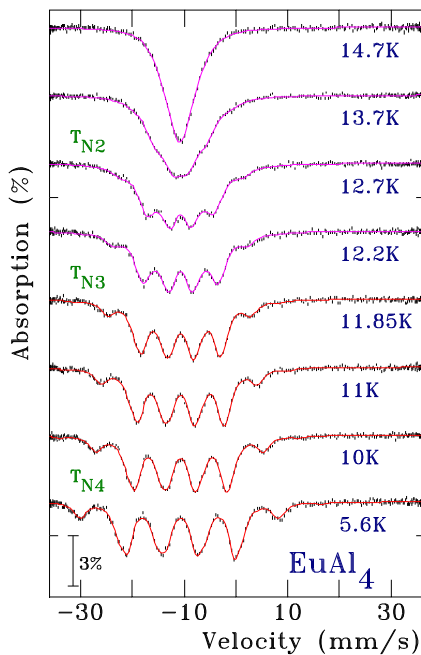
**FIG. 1.**  $^{151}\text{Eu}$  Mössbauer spectra for  $\text{EuGa}_4$  showing a simple reduction in  $B_{hf}$  on warming. Solid red lines show full Hamiltonian fits.<sup>9</sup>



**FIG. 2.** Temperature dependence of  $B_{hf}$  for  $\text{EuGa}_4$ . The solid magenta line is a fit to  $B_{hf}$  using a  $J = \frac{7}{2}$  mean-field function giving a transition temperature of  $T_N = 16.25(3)$  K.

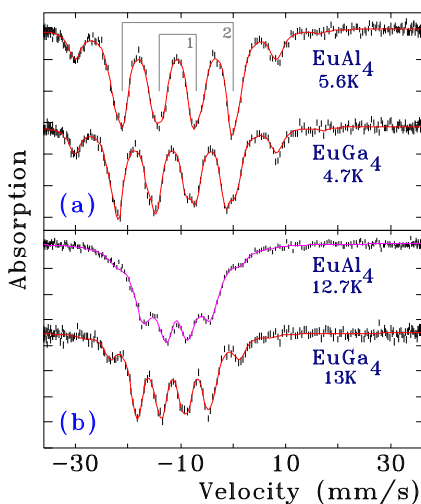
#### B. $\text{EuAl}_4$

Figure 3 shows that at 5.6 K,  $\text{EuAl}_4$  exhibits a well-split magnetic  $^{151}\text{Eu}$  Mössbauer spectrum with hyperfine parameters typical of a divalent europium system (listed in Table I). Despite  $\Delta$  being comparable to that seen in  $\text{EuGa}_4$ , we see no apparent contribution to the spectrum at 5 K. Figure 4(a) shows a direct comparison of the base-temperature  $\text{EuAl}_4$  and  $\text{EuGa}_4$  spectra. Working out from the centre at  $\sim -11$  mm/s, the inner pair (“1”) and the next pair



**FIG. 3.**  $^{151}\text{Eu}$  Mössbauer spectra for  $\text{EuAl}_4$  showing the evolution in form on warming. Solid red lines show full Hamiltonian fits for spectra taken below  $T_{N3}$  while the solid magenta lines show fits to an incommensurate modulation model above  $T_{N3} = 12.2$  K (more details in the text). The approximate locations of the four reported magnetic transitions are shown at the left.

out (“2”) each have the same shape and intensity, unlike the corresponding peaks in the spectrum of  $\text{EuGa}_4$ . The spectral linewidths observed at  $\sim 5$  K in  $\text{EuAl}_4$  and  $\text{EuGa}_4$  are essentially identical [1.19(2) and 1.13(2) mm/s respectively] so there is no evidence for a



**FIG. 4.** Comparison of the  $^{151}\text{Eu}$  Mössbauer spectra of  $\text{EuAl}_4$  and  $\text{EuGa}_4$  (a) at base temperature showing the effects of  $\Delta$  on the spectra, particularly for the two marked pairs; and (b) at an intermediate temperature where the impacts of the incommensurate modulation are apparent for  $\text{EuAl}_4$ . See text for more details.

distribution of  $\theta$ , that might wash out the effects of  $\Delta$ . A full Hamiltonian fit (using the  $\Delta$  taken from the paramagnetic state) yields an angle  $\theta$  between  $\vec{B}_{hf}$  and  $\vec{V}_{ZZ}$  of  $48(2)^\circ$ . This supports the neutron diffraction observation that the moments, at 4.3 K, have some in-plane component and are not fully oriented along the  $c$ -axis.<sup>5</sup> While, in principle, the switch from tetragonal to orthorhombic symmetry below  $T_{N3} = 12.2$  K<sup>1</sup> releases the  $\vec{V}_{ZZ}$  parallel to the  $c$ -axis constraint,  $\vec{V}_{ZZ}$  is still required to be parallel to *one* of the crystallographic axes so, even if the distortion were sufficient to change the direction of  $\vec{V}_{ZZ}$  the deduced magnetic structure would still be canted away from the  $c$ -axis and the (former)  $ab$ -plane.

The behaviour of  $\text{EuAl}_4$  on warming is as expected, more complex than that seen for  $\text{EuGa}_4$  (Fig. 3). This is made apparent immediately by comparing the 12.7 K spectrum of  $\text{EuAl}_4$  with the 13 K of  $\text{EuGa}_4$  in Fig. 4. Despite being measured at comparable fractions of  $T_N$ , the  $\text{EuGa}_4$  spectrum is clearly sharper and better resolved. All of the  $\text{EuAl}_4$  spectra taken above 12 K required the use of a modulated incommensurate model to fit them. In this model we assume that there is a distribution of hyperfine fields that results from an incommensurate modulation of the moment magnitudes,<sup>10,11</sup> and further assume that this modulation can be expressed in the form of Fourier harmonics,  $B_{k_1}$ ,  $B_{k_3}$ , etc. We introduce a constant term,  $B_{k_0}$ , to reduce the number of free parameters needed as the modulation approaches a square-wave form (or indeed, becomes commensurate). Variations of this model have been used to fit spectra for  $\text{EuPdSb}$ ,<sup>11</sup>  $\text{Eu}_4\text{PdMg}$ <sup>14</sup> and  $\text{Eu}(\text{Co}_{1-x}\text{Ni}_x)_{2-y}\text{As}_2$ ,<sup>15</sup> and more details can be found there. The results of these fits are shown as magenta lines in Fig. 3, and the amplitudes of the various Fourier components are plotted versus temperature in Fig. 5.

Starting with the lowest temperature behaviour, we find that the single-component full Hamiltonian model fits the data for  $T < 12$  K, and fitting the derived  $B_{hf}$  to a  $J = \frac{7}{2}$  mean-field model yields an extrapolated ordering temperature of 15.7(1) K, consistent with  $T_{N1}$ .<sup>4</sup> Above 12 K we find that the magnitude of the constant term ( $B_{k_0}$ ) drops abruptly, being replaced by the  $B_{k_1}$  and

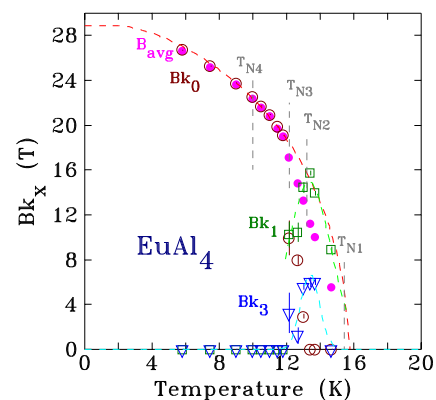


**FIG. 5.** Temperature dependence of the various hyperfine field ( $B_{hf}$ ) components fitted to the  $^{151}\text{Eu}$  Mössbauer spectra of  $\text{EuAl}_4$ . At the lowest temperatures only a single, uniform component,  $B_{k_0}$ , is present. Above  $T_{N3} = 12.2$  K an incommensurate modulation of the moments develops and additional Fourier components,  $B_{k_1}$  and  $B_{k_3}$  appear. Above  $T_{N1} = 15.4$  K all magnetic splitting is lost. Details of the fits are given in the text. The red dashed line is a fit to  $B_{avg}$  below  $T_{N3}$  using a  $J = \frac{7}{2}$  mean-field model giving an extrapolated transition temperature of  $T_N = 15.7(1)$  K.

$Bk_3$  Fourier components. It is possible that  $Bk_0$  should be zero, but replacing it by including higher-order harmonics such as  $Bk_5$  led to unstable fits. While we see no evidence for the lowest reported transition,  $T_{N4}$ , at 10 K, the clear break in behaviour at 12.0(2) K corresponds nicely with both with  $T_{N3}$ ,<sup>4</sup> and with the orthorhombic  $\rightarrow$  tetragonal structural transition that was reported to occur on warming through 12.2 K,<sup>1</sup> indicating that the formation of the incommensurate modulated magnetic structure is correlated with the change in crystallographic structure.  $T_{N2}$  at 13.4(2) K marks the temperature at which the amplitudes of the  $Bk_1$  and  $Bk_3$  Fourier components both peak, and  $Bk_0$  goes to zero, reflecting another significant change in nature of the magnetic order. Finally, all magnetic splitting is lost at  $T_{N1}$ . The estimated transition temperatures are listed in Table I.

#### IV. CONCLUSIONS

The isostructural intermetallic compounds  $\text{EuGa}_4$  and  $\text{EuAl}_4$  have been studied using  $^{151}\text{Eu}$  Mössbauer spectroscopy.  $\text{EuGa}_4$  exhibits relatively simple behaviour with transition to an antiferromagnetic state at 16.25(3) K with the moments oriented perpendicular to the  $c$ -axis. By contrast,  $\text{EuAl}_4$  exhibits a far more complex sequence of transitions. Starting at  $T_{N1} = 15.7(1)$  K, it enters an incommensurate sinusoidally modulated state which gradually squares up on cooling. The process is completed at  $T_{N3} = 12.0(2)$  K where the crystal structure also becomes orthorhombic. We find tentative evidence for the transition at  $T_{N2} = 13.4(2)$  K where the Fourier components reach their maximum amplitude and a constant term,  $Bk_0$ , appears. However we find no evidence for the lowest reported transition at  $T_{N4} = 10$  K.

#### ACKNOWLEDGMENTS

Financial support for this work was provided by Fonds Québécois de la Recherche sur la Nature et les Technologies, and the Natural Sciences and Engineering Research Council (NSERC) Canada. Work at Ames National Laboratory is supported by the Office of Basic Energy Sciences of the U.S. Department of Energy, Division of Materials Sciences and Engineering under Contract No. DE-AC02-07CH11358 with Iowa State University. B.K. is supported by the Center for the Advancement of Topological Semimetals (CATS), an Energy Frontier Research Center funded by the US DOE, Office of Basic Energy Sciences.

#### AUTHOR DECLARATIONS

##### Conflict of Interest

The authors have no conflicts to disclose.

#### Author Contributions

**D. H. Ryan:** Conceptualization (equal); Formal analysis (equal); Investigation (equal); Methodology (equal); Writing – original draft (equal); Writing – review & editing (equal). **Brinda Kuthanazhi:** Conceptualization (equal); Investigation (equal); Writing – review & editing (equal). **Na Hyan Jo:** Conceptualization (equal); Investigation (equal); Writing – review & editing (equal). **Paul C. Canfield:** Conceptualization (equal); Funding acquisition (equal); Investigation (equal); Methodology (equal); Resources (equal); Writing – review & editing (equal).

#### DATA AVAILABILITY

The data that support the findings of this study are available from the corresponding author upon reasonable request.

#### REFERENCES

- S. Shimomura, H. Murao, S. Tsutsui, H. Nakao, A. Nakamura, M. Hedo, T. Nakama, and Y. Ōnuki, *J. Phys. Soc. Jpn.* **88**, 014602 (2019).
- A. Nakamura, Y. Hiranaka, M. Hedo, T. Nakama, Y. Miura, H. Tsutsumi, A. Mori, K. Ishida, K. Mitamura, Y. Hirose, K. Sugiyama, F. Honda, R. Settai, T. Takeuchi, M. Hagiwara, T. D. Matsuda, E. Yamamoto, Y. Haga, K. Matsubayashi, Y. Uwatoko, H. Harima, and Y. Ōnuki, *J. Phys. Soc. Jpn.* **82**, 104703 (2013).
- T. Kawasaki, K. Kaneko, A. Nakamura, N. Aso, M. Hedo, T. Nakama, T. Ohhara, R. Kiyonagi, K. Oikawa, I. Tamura, A. Nakao, K. Munakata, T. Hanashima, and Y. Ōnuki, *J. Phys. Soc. Jpn.* **85**, 114711 (2016).
- A. Nakamura, T. Uejo, F. Honda, T. Takeuchi, H. Harima, E. Yamamoto, Y. Haga, K. Matsubayashi, Y. Uwatoko, M. Hedo, T. Nakama, and Y. Ōnuki, *J. Phys. Soc. Jpn.* **84**, 124711 (2015).
- K. Kaneko, T. Kawasaki, A. Nakamura, K. Munakata, A. Nakao, T. Hanashima, R. Kiyonagi, T. Ohhara, M. Hedo, T. Nakama, and Y. Ōnuki, *J. Phys. Soc. Jpn.* **90**, 064704 (2021).
- P. C. Canfield, T. Kong, U. S. Kaluarachchi, and N. H. Jo, *Philos. Mag.* **96**, 84 (2016).
- I. LSP Industrial Ceramics, Canfield crucible sets, 2022, <https://www.lspceramics.com/canfield-crucible-sets-2/> (accessed 24 August 2023).
- P. C. Canfield, *Reports on Progress in Physics* **83**, 016501 (2019).
- C. J. Voyer and D. H. Ryan, *Hyperfine Interact.* **170**, 91 (2006).
- A. Maurya, P. Bonville, A. Thamizhavel, and S. K. Dhar, *J. Phys.: Condens. Matter* **26**, 216001 (2014).
- P. Bonville, J. A. Hodges, M. Shirakawa, M. Kasaya, and D. Schmitt, *Eur. Phys. J. B* **21**, 349 (2001).
- Y. Homma, A. Nakamura, Y. Hirose, M. Hedo, T. Nakama, D. Li, F. Honda, Y. Ōnuki, and D. Aoki, *JPS Conf. Proc.* **3**, 011082 (2014).
- Mathematical instability in the fitting function for  $\theta \sim 90^\circ$  ( $90^\circ - \delta \equiv 90^\circ + \delta$ ) drives fits away from returning  $\theta = 90^\circ$ .
- D. H. Ryan, A. Legros, O. Niehaus, R. Pöttgen, J. M. Cadogan, and R. Flacau, *J. Appl. Phys.* **117**, 17D108 (2015).
- N. S. Sangeetha, S. Pakhira, D. H. Ryan, V. Smetana, A.-V. Mudring, and D. C. Johnston, *Phys. Rev. Mater.* **4**, 084407 (2020).